Balance between Coiled-Coil Stability and Dynamics Regulates Activity of BvgS Sensor Kinase in Bordetella

Elodie Lesne, Eva-Maria Krammer, Elena Dupre, Camille Locht, Marc Lensink, Rudy Antoine, Françoise Jacob-Dubuisson

▶ **To cite this version:**

Elodie Lesne, Eva-Maria Krammer, Elena Dupre, Camille Locht, Marc Lensink, et al.. Balance between Coiled-Coil Stability and Dynamics Regulates Activity of BvgS Sensor Kinase in Bordetella. mBio, 2016, 7 (2), pp.e02089. 10.1128/mBio.02089-15 . hal-03171779

HAL Id: hal-03171779
https://hal.univ-lille.fr/hal-03171779v1

Submitted on 17 Mar 2021

HAL is a multi-disciplinary open access archive for the deposit and dissemination of scientific research documents, whether they are published or not. The documents may come from teaching and research institutions in France or abroad, or from public or private research centers.

L'archive ouverte pluridisciplinaire **HAL**, est destinée au dépôt et à la diffusion de documents scientifiques de niveau recherche, publiés ou non, émanant des établissements d'enseignement et de recherche français ou étrangers, des laboratoires publics ou privés.

Distributed under a Creative Commons Attribution - NonCommercial - ShareAlike 4.0 International License

AMERICAN SOCIETY FOR MICROBIOLOGY | mBio®

RESEARCH ARTICLE

Balance between Coiled-Coil Stability and Dynamics Regulates Activity of BvgS Sensor Kinase in *Bordetella*

E. Lesne,[a] E.-M. Krammer,[b] E. Dupre,[a] C. Locht,[a] M. F. Lensink,[b] R. Antoine,[a] F. Jacob-Dubuisson[a]

Université de Lille, INSERM, CNRS, CHU Lille, Institut Pasteur de Lille, U1019-UMR 8204-CIIL, Centre d'Infection et d'Immunité de Lille, Lille, France[a]; Université de Lille, CNRS, UMR 8576-UGSF, Unité de Glycobiologie Structurale et Fonctionnelle, Lille, France[b]

E.-M.K. and E.D. contributed equally to this article.

ABSTRACT **The two-component system BvgAS controls the expression of the virulence regulon of *Bordetella pertussis*. BvgS is a prototype of bacterial sensor kinases with extracytoplasmic Venus flytrap perception domains. Following its transmembrane segment, BvgS harbors a cytoplasmic Per-Arnt-Sim (PAS) domain and then a predicted 2-helix coiled coil that precede the dimerization-histidine-phosphotransfer domain of the kinase. BvgS homologs have a similar domain organization, or they harbor only a predicted coiled coil between the transmembrane and the dimerization-histidine-phosphotransfer domains. Here, we show that the 2-helix coiled coil of BvgS regulates the enzymatic activity in a mechanical manner. Its marginally stable hydrophobic interface enables a switch between a state of great rotational dynamics in the kinase mode and a more rigid conformation in the phosphatase mode in response to signal perception by the periplasmic domains. We further show that the activity of BvgS is controlled in the same manner if its PAS domain is replaced with the natural α-helical sequences of PAS-less homologs. Clamshell motions of the Venus flytrap domains trigger the shift of the coiled coil's dynamics. Thus, we have uncovered a general mechanism of regulation for the BvgS family of Venus flytrap-containing two-component sensor kinases.**

IMPORTANCE **The two-component system BvgAS of the whooping cough agent *Bordetella pertussis* regulates the virulence factors necessary for infection in a coordinated manner. BvgS is the prototype of a family of sensor kinase proteins found in major bacterial pathogens. When BvgS functions as a kinase, *B. pertussis* is virulent, and the bacterium shifts to an avirulent phase after BvgS senses chemicals that make it switch to phosphatase. Our goal is to decipher the signaling mechanisms of BvgS in order to understand virulence regulation in *Bordetella*, which may lead to new antimicrobial treatments targeting those two-component systems. We discovered that the activity of BvgS is regulated in a mechanical manner. A short region of the protein that precedes the enzymatic domain switches between two states in response to signal perception by other BvgS domains. This switch region is conserved among BvgS homologs, and thus, the regulation uncovered here will likely be relevant for the family.**

Received 1 December 2015 **Accepted** 28 January 2016 **Published** 1 March 2016

Citation Lesne E, Krammer E-M, Dupre E, Locht C, Lensink MF, Antoine R, Jacob-Dubuisson F. 2016. Balance between coiled-coil stability and dynamics regulates activity of BvgS sensor kinase in *Bordetella*. mBio 7(2):e02089-15. doi:10.1128/mBio.02089-15.

Editor Scott J. Hultgren, Washington University School of Medicine

Copyright © 2016 Lesne et al. This is an open-access article distributed under the terms of the Creative Commons Attribution-Noncommercial-ShareAlike 3.0 Unported license, which permits unrestricted noncommercial use, distribution, and reproduction in any medium, provided the original author and source are credited.

Address correspondence to R. Antoine, rudy.antoine@pasteur-lille.fr, or F. Jacob-Dubuisson, francoise.jacob@ibl.cnrs.fr.

Widespread in eubacteria, two-component sensory transduction systems (TCSs) regulate many aspects of bacterial physiology in response to environmental stimuli, including major cellular programs like virulence, sporulation, or antibiotic resistance (1–3). Canonical TCSs are composed of a sensor kinase and a response regulator protein. Upon perception of a signal by the sensor domain, the kinase autophosphorylates and then transfers the phosphoryl group to the response regulator, triggering its activation (4). Unorthodox systems comprise additional proteins or domains involved in a phosphorelay, which is thought to allow a finer regulation in response to signals (5).

In the whooping cough agent *Bordetella pertussis*, the expression of the virulence regulon that is necessary for the colonization of the human respiratory tract is controlled by the TCS BvgAS (6, 7). BvgA is a classical response regulator, serving as a transcriptional activator of the virulence regulon when phosphorylated, and BvgS is a phosphorelay-containing histidine kinase (HK) receptor. BvgS forms a dimer (Fig. 1A). Each monomer is composed of two tandem periplasmic Venus fly trap (VFT) domains (Pfam SBP_bac_3), a transmembrane (TM) segment, and a cytoplasmic Per-Arnt-Sim (PAS) domain that are followed first by the typical dimerization and histidine phosphotransfer (DHp) and catalytic/ATP binding (CA) domains (Pfam HisKA and HATPase_c, respectively), which together form the HK domain, and then by receiver and histidine phosphotransfer (HPt) domains (8). BvgS is the prototype for a large family of poorly characterized VFT-containing HK receptors currently comprising more than 5,000 predicted members, notably in major bacterial pathogens, such as *Pseudomonas aeruginosa*, *Vibrio cholerae*, *Yersinia enterocolitica*, and *Borrelia burgdorferi* (9). A VFT domain is composed of two lobes joined by a hinge, which delimitate a pocket for the binding of a specific ligand (10). Clamshell motions allow reversible exchanges to occur between open and closed conformations. Typically, the binding of a ligand in the VFT cavity stabilizes the closed

Downloaded from http://mbio.asm.org/ on March 17, 2021 by guest

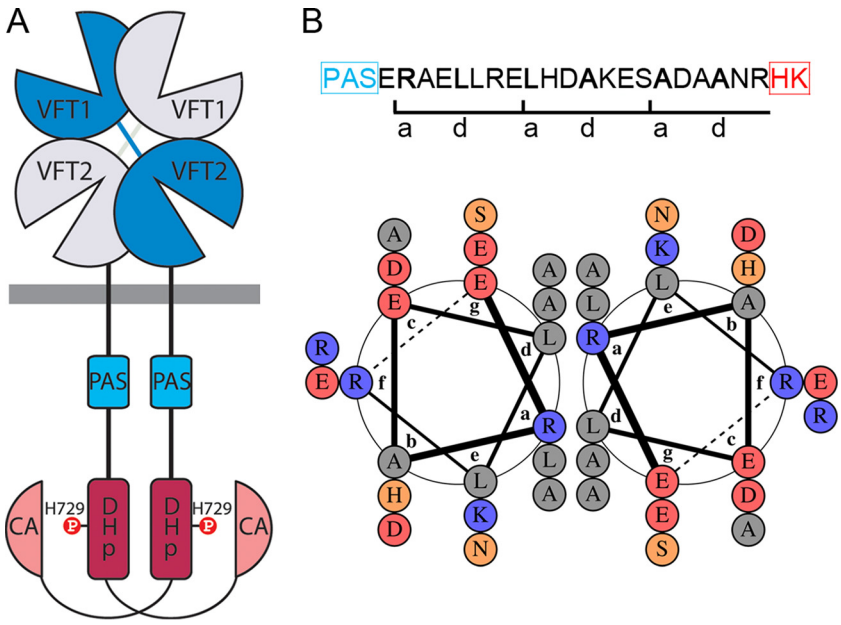

FIG 1 The PAS-HK linker of BvgS. (A) Schematic representation of the BvgS dimer. The receiver and HPt domains were omitted for clarity. The DHp domain, with the phosphorylatable His, and the catalytic and ATP-binding domains (CA) form the His kinase. (B) Amino acid sequence of the PAS-HK linker showing the a and d residues of the coiled coil, and representation by a helical wheel diagram using DrawCoil 1.0 (http://www.grigoryanlab.org/drawcoil/) as in reference 28. Hydrophobic residues are in grey, polar uncharged residues in orange, negative residues in red, and positive residues in blue. The abcdefg annotations correspond to the 3 heptads. PAS and HK represent the PAS and His-kinase domains, respectively.

conformation and triggers downstream cellular events, such as transport or signaling (10, 11).

BvgS is in a kinase mode of activity in the basal state at 37°C. In the laboratory, the addition of modulators, such as $MgSO_4$ or nicotinate, or conditions of low temperature or nutrient restriction shift the bacteria to the Bvg^-, avirulent phase (12–16). By using a Phos-Tag assay, we have shown that the dephosphorylation of BvgA is much faster after the addition of nicotinate to bacteria than when it occurs spontaneously, indicating that BvgS acts as a phosphatase in the Bvg^- phase (12). Nicotinate and its analogs are perceived by the membrane-proximal VFT domains of BvgS, and their binding appears to rigidify the entire periplasmic moiety (12, 17). The natural chemical signals that BvgS might perceive in the host and their site of action remain to be identified.

Recently, we described the crystallographic structure of the periplasmic moiety of BvgS (9). This structure reveals an intricate homodimer composed of two membrane-distal, N-terminal domains, termed "VFT1," in open conformations and two membrane-proximal, unliganded domains, termed "VFT2," in closed conformations. The VFT2 domains are followed by α-helices that likely continue across the membrane. We have shown that in the default state of BvgS, the periplasmic portion exerts a strain on the TM helices (9). This results in a conformation of BvgS in which the enzymatic moiety is in autokinase and phosphotransfer modes of activity (hereinafter referred to as the kinase state). The dynamics of the BvgS periplasmic moiety decreases after the perception of nicotinate, and the protein shifts to the phosphatase state (12). However, the molecular mechanisms of signal transduction are yet undeciphered.

The HK moiety of canonical bacterial HK receptors is dimeric (18–22). The DHp domains form a 4-helix bundle and harbor the phosphoacceptor His residues. The globular CA domains flank the DHp helices. The relative positions of the CA and DHp domains determine the reactions of autophosphorylation and phosphotransfer to a conserved Asp residue of the receiver domain or the reaction of dephosphorylation of the phosphoacceptor Asp residue (19, 23). HK receptors thus exist in two signaling states that are proposed to interconvert by remodeling of the DHp helical bundle (24, 25).

In BvgS, two long segments predicted to be α-helical (8) link the TM and PAS domains and the PAS and DHp domains, respectively (Fig. 1A). These two linkers are highly conserved among isolates of *B. pertussis* (26). The second is predicted to form a coiled coil (Fig. 1B). Canonical parallel 2-helix coiled coils (2-HCC) are left handed and composed of heptads whose residues, annotated as "abcdefg," form two helical turns (27). The a and d residues are generally hydrophobic and nonaromatic and are found at the interface of the two helices. The other residues are in general polar and favor the helix formation. The hydrophobic interface of the helices and ionic interactions both contribute to the coiled-coil stability (27–29). In this work, we focused on the 2-HCC preceding the enzymatic domain to decipher its role for signal transduction in BvgS, and we uncovered a mode of regulation that may apply to the family generally.

RESULTS

Effect of PAS-DHp linker length on kinase activity. In BvgS, the predicted coiled coil that precedes the DHp domain of the kinase is composed of three heptads (Fig. 1B). Five of six a and d positions of the three heptads are occupied by Ala or Leu residues. To test whether the register of the coil determines the enzymatic activity of BvgS, we introduced insertions or deletions therein, as previously described for a soluble HK receptor (30). We used as a template the sequence of a sensor kinase (EAW37541) from *Lyngbia*

Downloaded from http://mbio.asm.org/ on March 17, 2021 by guest

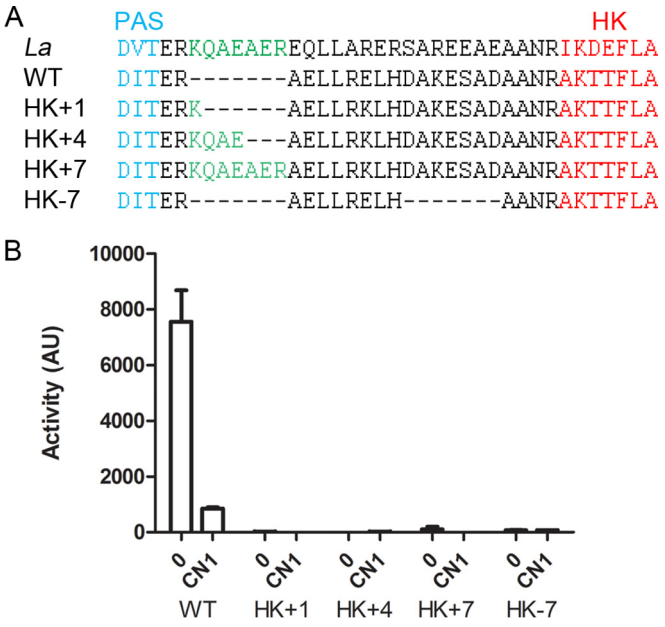

FIG 2 Effect of linker length on BvgS activity. (A) A sequence alignment of the junction between the PAS and DHp domains of the sensor kinase (EAW37541) from *Lyngbia aesturarii* strain PCC8106 (denoted *La*) and BvgS (denoted WT) is shown, with the sequences of the variants (denoted HK+1 to −7) underneath. (B) The *fha-lacZ* reporter was used to determine the activities of the BvgS variants compared to that of the wt strain under basal conditions (0) or after the perception of 1 mM chloronicotinate (CN1). The measurements were performed at least three times, and the means and standard errors of the means are indicated.

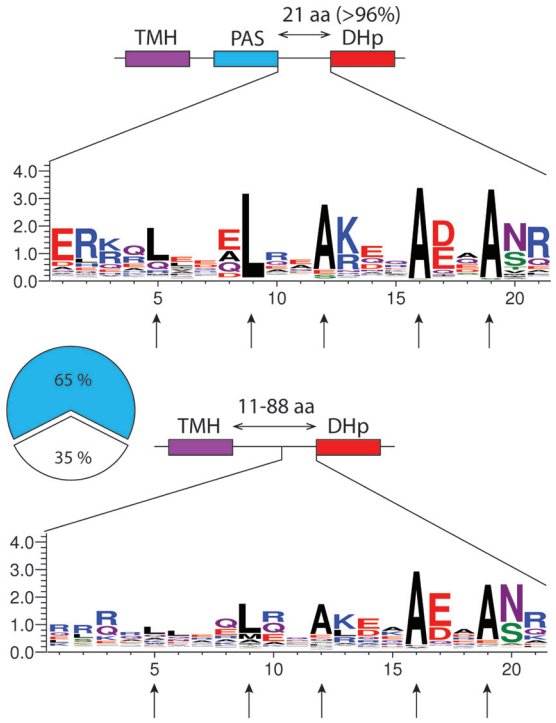

FIG 3 Conserved features of the segment preceding the DHp domain in the BvgS family. Top, schematic representation of the proteins with a PAS domain and sequence logo of the region encompassing the 2-HCC. TMH, transmembrane helix; aa, amino acids. In most proteins, the segment between the DIT motif that terminates the PAS domain and the AKS/TTFLAT motif that begins the DHp domain is 21 residues long. Bottom, schematic representation of the proteins with an α-helix between the TM segment and the DHp domain. The length of the linker varies widely between proteins; the logo is shown only for the last 21 residues. The vertical arrows indicate the LLAAA motif.

aesturarii strain PCC8106, whose linker is highly similar to that of BvgS but with an additional heptad (Fig. 2A). Thus, we inserted the 7 intervening residues of the *L. aesturarii* sensor kinase (EAW37541) into BvgS to lengthen the linker by two helical turns while preserving the coil register. We also added 1 or 4 residues of *L. aesturarii* sensor kinase (EAW37541) to the BvgS linker, which is anticipated to shift the register of the coiled coil by 100° or 40°, respectively. The three *bvgS* variants were introduced into *B. pertussis* by allelic exchange, and the transcriptional fusions *ptx-lacZ* and *fhaB-lacZ* were used as reporters to determine the activity of the BvgS variants. Transactivation of the *ptx* and *fhaB* promoters requires high and low concentrations of phosphorylated BvgA, respectively (31), and therefore, the *fhaB-lacZ* fusion is used to detect low BvgS activity levels. In contrast to wild-type (wt) BvgS, none of the three BvgS modifications resulted in detectable β-galactosidase (β-Gal) activity using either reporter system (Fig. 2B; also data not shown). To verify that the BvgS variants were present in the cells, we performed immunoblot analyses of membrane extracts of the various recombinant strains. The variants were detected, albeit at low levels, suggesting a less efficient biogenesis or an increased tendency to degradation (see Fig. S1A in the supplemental material).

To determine whether the PAS-kinase linker is conserved in the BvgS family, we aligned the sequences of more than 1,000 representative BvgS homologs, i.e., sensor kinases that harbor 2 VFT domains, irrespective of their phosphorelay type. Approximately 65% of the putative proteins harbor signatures of one or several PAS domain(s) between the TM segment and the DHp domain of the kinase, and the other 35% harbor a predicted α-helix all the way from the TM segment to the DHp domain (Fig. 3). In BvgS, the segment between the Asp-Ile-Thr (DIT) motif that terminates the PAS domain and the Ala-Lys-Ser/Thr-Thr (AKS/TT) motif that begins the DHp domain is 21 residues long. Remarkably, 96% of the corresponding segments in PAS-containing homologs are also composed of 21 residues with three putative heptads. The composition of that region is conserved in the family (Fig. 3). We thus also tested the effect of deleting a complete heptad from BvgS (Fig. 2A). The resulting recombinant *B. pertussis* strain also expressed no β-Gal activity (Fig. 2B), even though the latter modification did not impair the production of BvgS or its localization to the membrane (see Fig. S1B in the supplemental material). Altogether, these data support a mechanical role for that region.

Topology and dynamics of the coil. To map the contacts between the two helices that compose the putative 2-HCC of BvgS, we performed a Cys-scanning analysis in *Escherichia coli* using a truncated BvgS variant devoid of the receiver and HPt domains and harboring a C-terminal 6-His tag. This shorter form, with a molecular weight of 95 kDa, has 2 natural Cys residues, Cys607 and Cys881, in the PAS and CA domains, respectively, instead of the 5 in full-length BvgS. As the truncated protein spontaneously forms a moderate proportion of disulfide (S-S) bond-mediated dimers (see Fig. S2A in the supplemental material), we replaced Cys607 and Cys881 with Ala and Ser, respectively. These sub-

Downloaded from http://mbio.asm.org/ on March 17, 2021 by guest

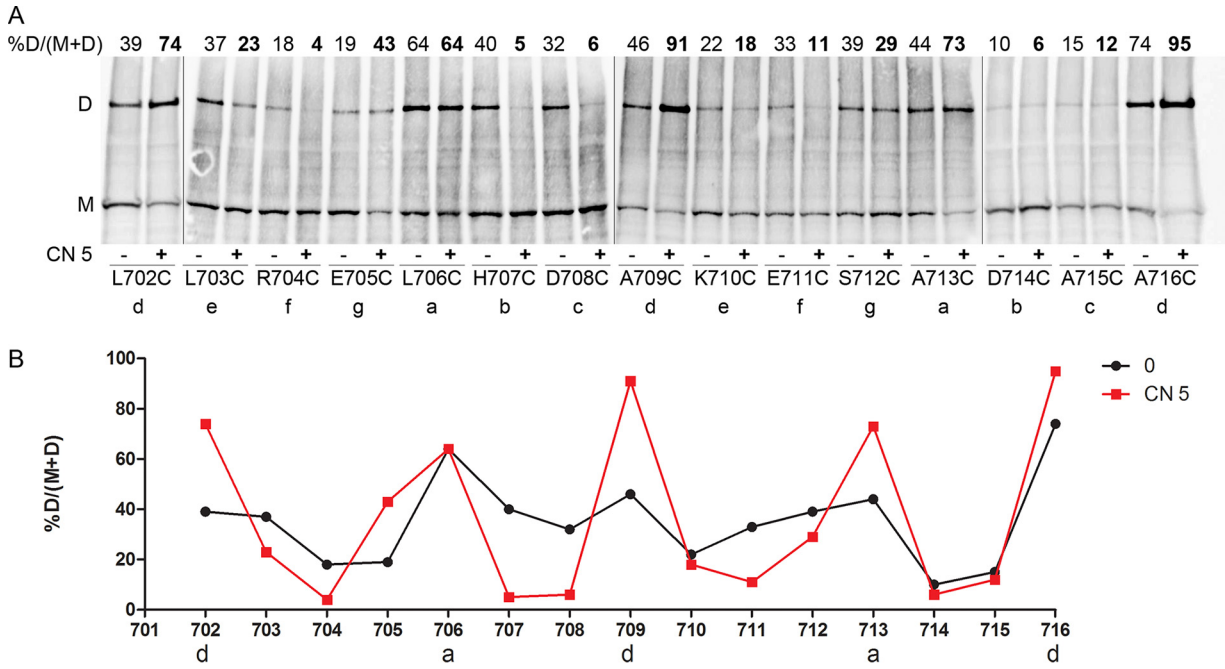

FIG 4 Topology and dynamics of the PAS-HK linker. (A) Cys-scanning analyses for the BvgS^{t} variants were performed under basal conditions (−) or after the addition (+) of 5 mM chloronicotinate (CN 5). The monomeric and dimeric forms of BvgS^{t} are denoted M and D, respectively. The a to g positions of the 2-HCC heptads are indicated below each substitution. The proportions of dimers, determined as indicated at the top left, are given at the top of each lane. BvgS^{t} was detected using anti-His tag antibodies. (B) The results of a representative experiment have been graphed to facilitate reading. The proportions of dimers are shown under basal condition (0, black curve) or after the perception of chloronicotinate (CN 5, red curve).

stitutions were also introduced into full-length BvgS ($BvgS_{C607A+C881S}$) to determine the activity of the variants in *B. pertussis*. Full-length $BvgS_{C607A+C881S}$ (hereinafter called BvgS^{fl}) showed a reduced sensitivity to nicotinate but was modulated by a more potent modulator, chloronicotinate (see Fig. S2B). The corresponding truncated form of $BvgS_{C607A+C881S}$ is called BvgS^{t}. Residues Leu702 to Ala716 were individually replaced with Cys in BvgS^{t} for the Cys-scanning analysis (Fig. 4A and B), and in BvgS^{fl}, they were replaced with Cys to measure the effect of each substitution on activity (Fig. S2C and D).

Intradimer S-S bond formation was determined after treating the bacteria with an oxidant, copper-*o*-phenanthroline. Following electrophoresis of the bacterial membrane extracts under nonreducing conditions, dimer proportions were determined by densitometry analyses of immunoblots. In their basal, kinase state, many BvgS^{t} variants formed dimers (Fig. 4A and B). Somewhat higher proportions of dimers were detected with Cys at positions 706, 709, 713, and 716, corresponding to the a and d positions of the putative 2-HCC, as well as with Cys at positions 703, 707, 708, and 712, flanking the a and d residues. These results support the prediction of a 2-HCC for this region. They also indicate that the kinase state of BvgS is characterized by considerable dynamics of this 2-HCC.

All the recombinant *B. pertussis* strains with the BvgS^{fl} variants expressed detectable β-Gal reporter activity, except for the $BvgS^{fl}_{A713C}$ variant (see Fig. S2C and D in the supplemental material). Detection of BvgS^{fl} in *B. pertussis* membrane extracts was performed for the variants with no or low activity to check protein production and stability (see Fig. S1C). $BvgS^{fl}_{A713C}$ was produced in normal amounts, indicating that this Ala residue is critical for function and consistent with the observation that the a position of the third heptad is invariant in the family (Fig. 3). $BvgS^{fl}_{R704C}$ was hardly detected, and $BvgS^{fl}_{E711C}$ was found in small amounts, suggesting that the corresponding substitutions affect BvgS biogenesis or susceptibility to degradation. Regarding their responses to the modulator, several variants were less sensitive than the control, but they all responded to chloronicotinate, except for the $BvgS^{fl}_{A716C}$ variant (Fig. S2C). Notably, Ala716 corresponds to the d position of the third heptad, and this residue is also highly conserved in the family.

We then determined the topology and dynamics of the linker for BvgS^{t} variants in the phosphatase state by treating the bacteria with 5 mM chloronicotinate for 30 min before adding the oxidant. The Cys-scanning analyses showed that, for the a and d positions of the 2-HCC, the dimer proportions were much higher in the modulated, phosphatase state than in the kinase state (Fig. 4A and B). In contrast, considerably lower dimer proportions were found at the positions of the 2-HCC predicted to not form the interface of the two helices. Thus, in the phosphatase state, BvgS adopts a more rigid conformation in that region, with the 2-HCC realized as predicted. This conformation maximizes interactions between the conserved Leu and Ala residues at the interface of the helices. The limited movements of the coiled coil in that state contrast with its marked rotational dynamics in the kinase state.

Alterations to coil stability affect BvgS function. The LXXXLXXAXXXAXXA motif (hereinafter denoted LLAAA), whose Leu and Ala residues are at the a and d positions of the 2-HCC, precedes the DHp domain and is conserved among BvgS homologs with a PAS domain (Fig. 3). Our Cys-scanning data indicate that this motif contributes to regulating BvgS activity. To confirm its function, those conserved residues were replaced both *in vivo* and *in silico*. Thus, the 2-HCC was made into a *bona fide*

Downloaded from http://mbio.asm.org/ on March 17, 2021 by guest

leucine zipper by progressively replacing the three Ala residues with Leu residues, and conversely, the two Leu residues of the motif were replaced by Ala residues to loosen its hydrophobic interface (Fig. 5A). *In silico*, we generated 10 models for each of the 6 sequences of the Arg699–Ala719 segment with the CCbuilder program and determined for each variant the value of the energy of interaction per residue using the Coilcheck+ program (Fig. 5B). As anticipated, the progressive introduction of Leu residues led to a stepwise stabilization of the coiled coil, which is expected to favor the phosphatase state. The *in silico* replacement of one or several Leu residues with Ala residues had the inverse effect, leading to configurations with lower energies of interaction between the two helices, expected to have opposite consequences for BvgS activity.

The activities of the BvgS variants were determined in *B. pertussis*. The Ala709Leu substitution at the d position of the second heptad yielded a BvgS variant (LLLAA) that was more sensitive to modulation than its wt counterpart, and variants with two or three additional Leu residues (LLLLA and LLLLL) expressed no kinase activity, being presumably locked in the phosphatase state (Fig. 5C; see also Fig. S3 in the supplemental material). BvgS was detected to wt levels in the membrane for those two variants, ruling out a problem of protein structure or stability (see Fig. S1D). Thus, the 2-HCC with four or five leucines in central a and d positions is likely too stable to allow the kinase state of activity. The partial effect of the single A709L substitution (LLLAA variant) might be explained by a marginally more stable coiled coil than that of the wt protein, triggering the shift to the phosphatase state at lower modulator concentrations. Conversely, variants with 4 or 5 alanines in the 2-HCC (LAAAA and AAAAA variants) were unresponsive to the modulators, even at high concentrations (Fig. 5D). The coiled coil with these modifications may be too loose to achieve or to maintain the phosphatase state upon perception of the modulators.

The PAS domain is dispensable for BvgS activity. Approximately 35% of sensor kinases in the BvgS family lack a PAS domain and instead have predicted α-helices from the TM segment to the DHp domain of the kinase (Fig. 3). The length of that helix, from the first residue after the predicted TM segment to the beginning of the DHp domain, varies from 11 to 88 residues. Notably, 2-HCCs are predicted in the region immediately preceding the DHp domain, with the LLAAA motif generally present (Fig. 3).

To gain insight into the role of the PAS domain for BvgS regulation, we deleted it, using as a template the PAS-less sequence of a BvgS homolog, the sensor kinase (PP3413; GI:24985059) of *Pseudomonas putida*. The linker of the PP3413 protein has the most common length among PAS-less BvgS homologs and a complete LLAAA motif. Although three different deletions, $\Delta(R_{585}–A_{700})$ (deletion of the sequence from Arg585 to Ala700), $\Delta(M_{584}–A_{700})$, and $\Delta(F_{583}–A_{700})$, were introduced in an attempt to reconnect the flanking helices in a functional manner, none of these BvgS variants expressed kinase activity (see Fig. S4A and B in the supplemental material). The three variants were found in small amounts in *B. pertussis*, suggesting that the protein was improperly assembled or degraded (see Fig. S1E). These results suggest that the regions upstream and downstream from the PAS domain in BvgS have not evolved to function together in the absence of a PAS domain.

Thus, to improve the construct, we inserted the entire portion between the TM segment and the DHp domain of the PP3413 protein in place of the BvgS PAS region. Three additional chimera of different lengths were constructed similarly, using the sequences of other PAS-less family members (Fig. 6A). The smaller two variants, $BvgS_{\Delta PAS\text{-}R1}$ and $BvgS_{\Delta PAS\text{-}R2}$, gave high levels of reporter activity in *B. pertussis* but were unresponsive even to high concentrations of the stronger modulator, chloronicotinate, indicating that they were locked in the kinase state (Fig. 6B). In contrast, $BvgS_{\Delta PAS\text{-}R4}$ responded to nicotinate and chloronicotinate, although it was somewhat less sensitive than wt BvgS, and $BvgS_{\Delta PAS\text{-}R3}$ gave an intermediate phenotype. Therefore, it is possible to generate PAS-less BvgS variants that are in the kinase state by default and shift to the phosphatase state in response to modulation, demonstrating that the PAS domain is dispensable for BvgS function. Under those conditions, a long linker between the membrane and the HK domain appears to facilitate the shift to the phosphatase state (Fig. 6B). Note that the larger $BvgS_{\Delta PAS\text{-}R4}$ chimera harbors additional heptads that are likely to strengthen the interface of the 2-HCC. We calculated the energy of interaction per residue for the 4 linkers of different lengths using Coilcheck+ (see Fig. S5). The R3 and R4 linkers had considerably lower energies of interaction per residue, indicating that they adopt the stable 2-HCC conformation more readily than the two shorter ones, consistent with their responses to modulation.

Coiled-coil stability determines BvgS function in the absence of the PAS domain. As the LLAAA motif is conserved in the BvgS family members that are devoid of a PAS domain, we tested the effects of altering the hydrophobic interface of the 2-HCC in the unresponsive $BvgS_{\Delta PAS\text{-}R1}$ variant using principles similar to those revealed for BvgS. Our rationale was that a Leu zipper-like interface might favor the phosphatase state by increasing coil stability. The three Ala residues of the motif were replaced successively with Leu (Fig. 7A). The $BvgS_{\Delta PAS\text{-}R1\text{-}1L}$ variant (having 1 Ala-to-Leu substitution) was active and responded to the modulator (Fig. 7B), although it was less sensitive than the wt protein. For the $BvgS_{\Delta PAS\text{-}R1}$ variants with 2 or 3 additional leucines, no β-Gal activity was detected using the *ptx-lacZ* reporter (Fig. 7B) and hardly any using the *fhaB-lacZ* reporter (see Fig. S3B in the supplemental material). The production of those variants in *B. pertussis* was similar to that of wt BvgS (see Fig. S1F). Thus, marginally increasing the stability of the 2-HCC interface facilitates the response of $BvgS_{\Delta PAS\text{-}R1}$ to modulation, while constraining the coil in its low-energy conformation locks BvgS into the phosphatase mode. Therefore, the same rules of kinase regulation prevail irrespective of the presence of a PAS domain.

Nevertheless, as the short R1 linker sequence occurs naturally in a BvgS homolog, we hypothesized that it regulates the enzymatic activity of its own sensor kinase in response to the closing of the VFT domains of that protein. In BvgS, closing the VFT1 domains with an S-S bond to mimic the binding of putative ligands shifts the protein to the phosphatase state (9). Introducing the same Cys substitutions into the $BvgS_{\Delta PAS\text{-}R1}$ and $BvgS_{\Delta PAS\text{-}R1\text{-}1L}$ variants affected the activity of $BvgS_{\Delta PAS\text{-}R1}$ and almost totally abolished that of $BvgS_{\Delta PAS\text{-}R1\text{-}1L}$ (Fig. 7C). Thus, closing VFT1 triggers the full shift to the phosphatase state if the 2-HCC hydrophobic interface of the short variant is marginally strengthened by an additional Leu. This shows that the short linker is functional in response to clamshell-like VFT closing motions.

Downloaded from http://mbio.asm.org/ on March 17, 2021 by guest

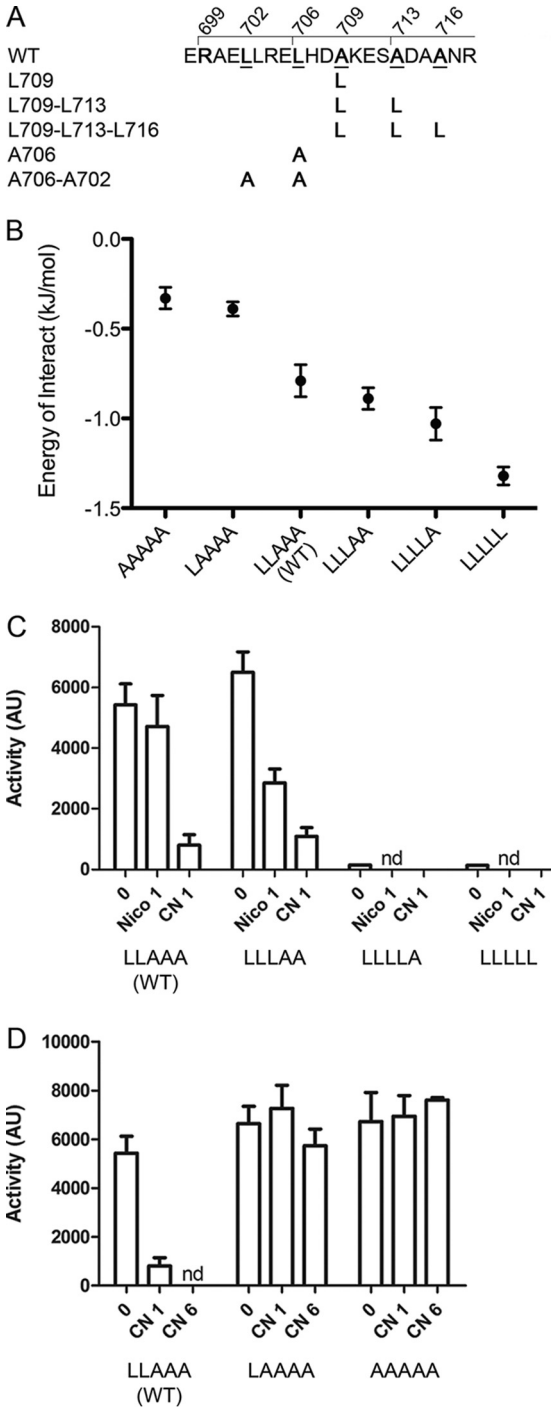

FIG 5 Coiled-coil stability determines BvgS activity. (A) Sequence of the PAS-HK linker and substitutions introduced to modify the 2-HCC interface. The wt LLAAA motif is underlined. (B) Impact of the mutation(s) on the interaction energy of the helices in the 2-HCC as determined *in silico*. The values for pseudoenergy of interaction per residue were calculated for the wt 2-HCC and its variants harboring modifications of the LLAAA motif. Each value represents the average of the values obtained from 10 models for each coil sequence, and the errors of the means are given. (C) Activities of the BvgS variants with Ala-to-Leu substitutions determined using the *ptx-lacZ* reporter. Two modulators were used, nicotinate (Nico) and chloronicotinate (CN), each at 1 mM. Note that also with the *fha-lacZ* reporter, no activity was detected for $BvgS_{L709\text{-}L713}$ and $BvgS_{L709\text{-}L713\text{-}L716}$ (LLLLA and LLLLL variants) (see Fig. S3A in the supplemental material). nd, not determined. (D) Activities

(Continued)

DISCUSSION

The enzymatic moiety of BvgS harbors the same DHp and CA domains as those of canonical TCS sensor kinases, but in many other aspects, BvgS differs from the latter (8). First, instead of extracytoplasmic PAS-like PDC sensor domains, BvgS harbors VFT perception domains of the type found in transport systems (32). Second, each monomer in BvgS harbors a single transmembrane segment, while two TM segments flank the extracytoplasmic PDC sensor domains. Third, canonical sensor kinases frequently harbor a HAMP domain between the TM and DHp domains, while HAMP domains are not found in the BvgS family (our unpublished observations). Instead, BvgS and its homologs harbor between the TM and DHp domains one or several cytoplasmic PAS domains or, in rare cases, a GAF domain, followed by one predicted α-helix per monomer or, for those that have no PAS or GAF domain, only one α-helix per monomer. All those features and the dynamics of VFT domains, which close by clamshell motions in response to ligand binding, have led us to propose that sensor kinases of the BvgS family regulate their activity along distinct mechanistic principles (9). This study shows that the linker upstream from the kinase moiety of BvgS is organized as a coiled coil of two parallel α-helices. The kinase or phosphatase activity of the protein depends on whether this 2-HCC is flexible and dynamic or whether it is rigid and adopts the low-energy conformation dictated by its hydrophobic interface.

BvgS is active as a kinase in its basal state, and the perception of specific chemicals by the VFT domains triggers the shift to a phosphatase state (12). While a kinase state by default might not be a general feature among BvgS homologs (33), we show here that the 2-HCC immediately preceding the DHp domain is a functionally essential determinant in the family. The length and the interface of this 2-HCC are critical for BvgS activity. In particular, the behavior of the coiled coil determines the enzymatic activity of the protein. Thus, a dynamic, flexible 2-HCC favors the kinase state, while the phosphatase state is favored when the 2-HCC adopts the more rigid conformation that buries its hydrophobic interface. The rules deciphered here appear to apply irrespective of the presence of a PAS domain. The PAS domain itself may therefore be an additional but dispensable element of regulation.

As a general rule, the length and composition of a 2-HCC determine its stability. Typical examples of highly stable 2-HCC are Leu zippers, common structural motifs that serve as determinants of dimerization (34). In the BvgS family, the conserved LLAAA motif confers a marginal stability on the 2-HCC, and remarkably, one can manipulate the equilibrium between the two states by modifying these critical residues. Thus, with 5 leucines, the 2-HCC resembles a Leu zipper, which locks the protein in the phosphatase state. In contrast, with 5 Ala residues, the flexibility and dynamics of the coiled coil keep the protein in the kinase state. The effects of these replacements are reflected in their energy variations, showing an increasing stabilization with an increasing number of Leu residues in the motif. The occurrence of two states for BvgS and the ability to shift from one state to the other thus require that the stability of the coiled-coil interface remain within

Figure Legend Continued

for the Leu-to-Ala mutants were determined using the *ptx-lacZ* reporter. Chloronicotinate at 1 mM or 6 mM was used as the modulator. (C and D) The means and standard errors of the means are given.

Downloaded from http://mbio.asm.org/ on March 17, 2021 by guest

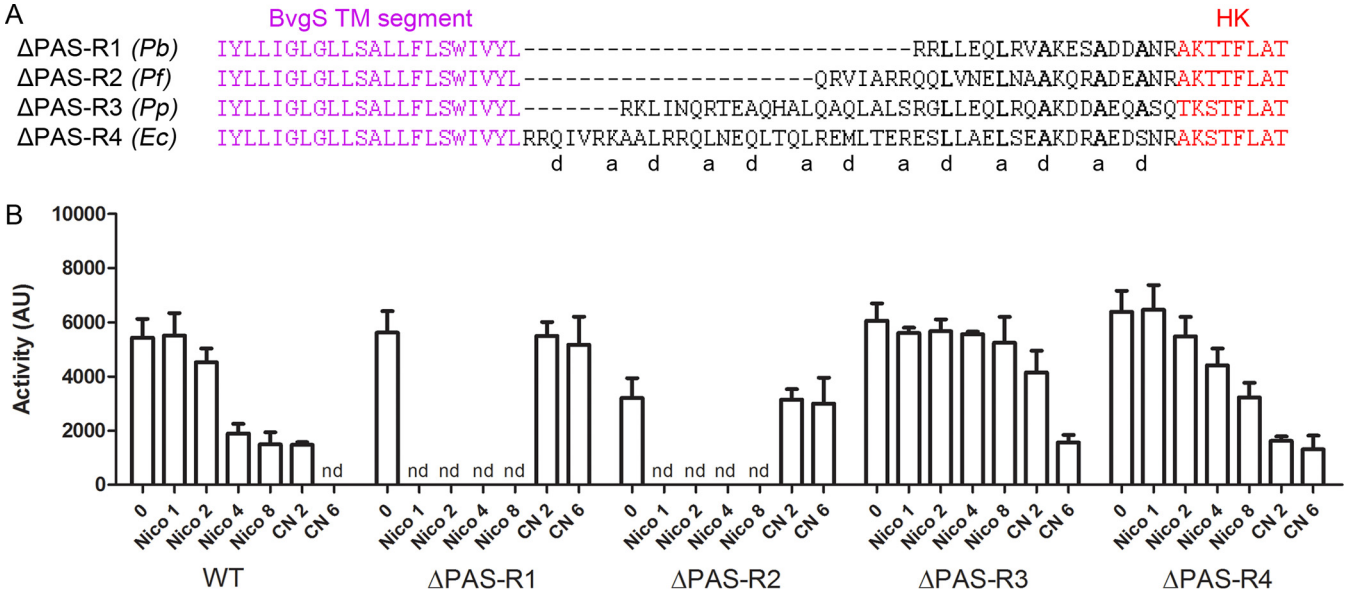

FIG 6 Chimeric BvgS variants with natural linkers of homologs. (A) Sequences of the variants in which the region between the TM segment and the DHp domain of BvgS was replaced with natural linkers of PAS-less BvgS homologs. The species from which the sequences originate are indicated, as follows: *Pb*, *Pseudomonas brassicacearum* (GI:742884217); *Pf*, *Pseudomonas fragi* (GI:515153750); *Pp*, *Pseudomonas putida* (GI:24985059); and *Ec*, *Enterobacter cloacae* (GI:915610361). The variants obtained were named ΔPAS-R1, -R2, -R3, and -R4, respectively. The first 4 residues of the DHp domain originate from the respective homolog, followed by the BvgS sequence from the FLAT motif on. (B) The *ptx-lacZ* reporter was used to determine the basal activities and the responses to nicotinate (Nico) and chloronicotinate (CN) (at the indicated millimolar concentrations) of the $BvgS_{\Delta PAS}$ variants compared to those of wt BvgS (WT). The means and standard errors of the means are given. nd, not determined.

specific limits. Interestingly, the stabilization and destabilization of the linker preceding the HK domain were recently shown to also control the signaling state of DesK, a very different type of TCS sensor kinase (35).

The Cys-scanning analyses show that strong dynamics of the PAS-HK linker corresponds to the kinase state and that the more rigid, stable conformation of the 2-HCC corresponds to the phosphatase state. Interestingly, recent reports point to a conforma-

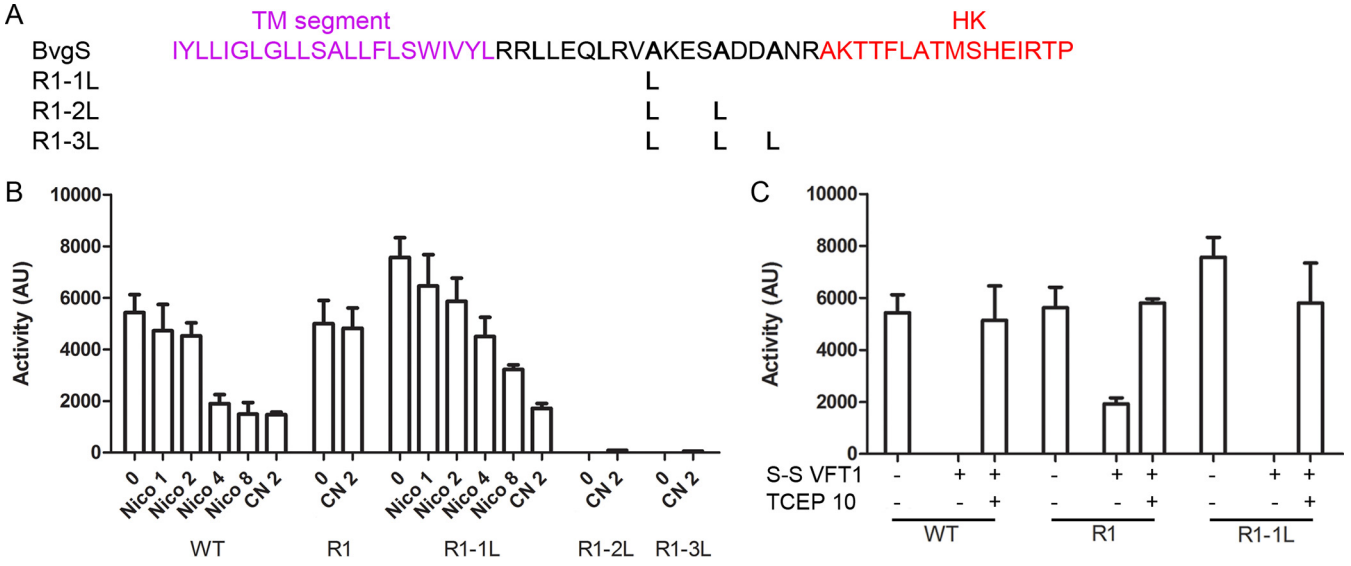

FIG 7 Regulation of BvgS in the absence of the PAS domain. (A) Sequence of the linker of $BvgS_{\Delta PAS\text{-}R1}$ and substitutions introduced to affect coiled-coil stability. The variants are denoted R1-1L, R1-2L and R1-3L to indicate the presence of 1, 2, or 3 Ala-to-Leu substitutions, respectively. (B) The *ptx-lacZ* reporter was used to determine the activities of $BvgS_{\Delta PAS\text{-}R1}$ and its variants. The *fhaB-lacZ* reporter also did not result in any activity being detected for the variants with 2 or 3 additional Leu residues (see Fig. S3B in the supplemental material). (C) Effect of introducing an S-S bond between the lobes of the VFT1 domain on the activities of wt BvgS (WT) and the indicated variants using the *ptx-lacZ* reporter, compared with the activities of the corresponding variants without the S-S bond. Where indicated, the reducing agent TCEP [tris(2-carboxyethyl)phosphine] was added to the cultures at 10 mM for the last 6 h to reduce the S-S bond in VFT1. The means and standard errors of the means are given.

Downloaded from http://mbio.asm.org/ on March 17, 2021 by guest

tional and dynamic asymmetry of the DHp helices in the kinase mode of activity of canonical HKs (18, 20, 22). An asymmetric helical bending in the DHp domain indicates that only one monomer catalyzes autophosphorylation at a time, and a sequential flip-flop between monomers has thus been proposed (18). In that model, a symmetrical, rigid DHp domain corresponds to the phosphatase state. If this model holds true for BvgS, it is tempting to speculate that its 2-HCC and DHp domain are part of the same functional unit, which is dynamic in the kinase state. According to this scenario, after perception of the modulator by the VFT domains, the 2-HCC adopts a stable conformation dictated by its hydrophobic interface. This rigidifies the DHp domain, resulting in a shift of activity to the phosphatase state.

The PAS domain of BvgS can be functionally replaced by specific linker sequences of PAS-less BvgS homologs, and notably, the rules of BvgS regulation are similar with or without a PAS domain. Thus, the replacement of one Ala by Leu in the LLAAA coiled-coil motif of the nicotinate-unresponsive $BvgS_{\Delta PAS\text{-}R1}$ variant restores its response to the modulator and to the closing of VFT1, and additional Ala-to-Leu replacements lock it in the phosphatase state, as for its wt BvgS counterpart. This demonstrates that irrespective of the presence of a PAS domain, regulation of kinase activity in the BvgS family implies transitions between two states of the coil preceding the enzymatic domain: a dynamic state in the kinase mode and a more rigid state in the phosphatase mode.

In the context of the BvgS sequence, however, not all linkers of PAS-less homologs confer upon BvgS the proper regulation. Thus, only the longer variants were responsive to modulation. This is consistent with the coiled coil's interaction energy increasing with the coil length. In the context of the BvgS sequence, the small values of interaction energy for the short 2-HCCs from homologs might be insufficient to lock them in the stable conformation required for phosphatase activity in response to the nicotinate signal, thus allowing a degree of dynamics. However, a marginally more stable 2-HCC harboring one additional Leu residue, combined with the closing of the VFT1s to mimic the presumed binding of a ligand in the natural situation, triggers the shift. In addition to length, the composition of the coiled coil and of its flanking sequences most likely also contributes to regulation. Interestingly, in the BvgS family, the segment immediately following the TM helix generally harbors several charged residues (our unpublished observations). How the properties of this linker region affect its function remains to be established. Notably, spontaneous point mutations in that region make BvgS unresponsive to modulation, supporting its role in the regulation of activity, and a similar observation was also made for a homolog, EvgS (36–38).

Although the PAS domain appears to be dispensable, its sequence in BvgS is remarkably conserved in the species that compose the *Bordetella bronchiseptica* complex, arguing that it contributes to BvgS function (26). This is supported by the observation that many spontaneous substitutions that freeze BvgS or EvgS in the kinase state map to the PAS domain or to the α-helical region that precedes it (36–38). BvgS exists in two states that are in thermodynamic equilibrium (12). The integrity of the PAS core is important for BvgS regulation, which has led us to propose a mechanical role for this domain (39). Our hypothesis is that the PAS domains in the BvgS dimer have distinct interfaces in the two states of activity. According to that model, their specific interface in the kinase state might prevent the coiled coil below from adopting its hydrophobic interface, and thus, the coil remains dynamic. Signal perception by the periplasmic domain might trigger a shift of the PAS domains' interface, and this modified PAS arrangement is compatible with the low-energy, rigid conformation of the coiled coil. The PAS domain may thus serve as a toggle switch that determines the conformation and dynamics of the linker below. A related model has been proposed for EvgS (38). In addition, it is possible that the PAS domain is also involved in sensing. It has been shown that nutrient availability affects BvgS activity (16). Specific molecules reflecting the metabolic state of the bacterium might be picked up by the PAS cavity and influence the regulation that we propose here.

Several other linkers occur in BvgS. Those between the HK and receiver domains and between the receiver and HPt domains of BvgS are poorly conserved and predicted to be unstructured (26). Signal transmission between the latter domains is most likely mediated by direct protein-protein interactions (21, 40), with the linkers serving solely to ensure spatial proximity between domains and, thus, to maintain their high local concentrations. In contrast, the TM domain and the linker preceding the PAS domain are predicted to form a long, continuous α-helix. The sequence of this linker is virtually invariant among isolates of *B. pertussis* (26) and conserved among BvgS homologs harboring a PAS domain. The signal transmission from the periplasmic domains to the kinase must depend on conformational changes of these helices as well. It will be interesting to decipher how this linker participates in signal transmission in order to construct a model for signaling in BvgS, from the periplasmic domains to the HK domains.

MATERIALS AND METHODS

Strains and plasmids. *B. pertussis* was grown on Bordet-Gengou agar plates for 2 days at 37°C and then cultured in modified Stainer-Scholte (SS) liquid medium at 37°C under agitation. Recombinant strains were constructed as described previously (9, 26). The transcriptional fusions used as reporters were described previously (41). The pPORVPH plasmid used for the Cys-scanning analysis encodes $BvgS^t$ with a C-terminal His tag for detection in *E. coli*. It is based on the previously described plasmids pFc3 (42) and pGEV-VFT1+2 and pUCmosaic (17). A detailed description of the construction of the plasmids used in this work and of the introduction of mutations is provided in Text S1 in the supplemental material.

Protein sequence analyses. The NR database release of 14 October 2015 (73,037,689 sequences) was downloaded from the National Center for Biotechnology Information (NCBI). To identify putative sensor kinases of the BvgS family, we searched the NCBI protein database using the hmmsearch program from the HMMER package (http://hmmer.org/) (43) and the profile hidden Markov models PF00497 for the bacterial extracellular solute-binding protein (family 3) (http://pfam.wfam.org/family/PF00497/hmm) and PF00512 for the His kinase A domain provided by the Pfam database (http://pfam.wfam.org/family/PF00512/hmm) (44). Further details are provided in Text S1 in the supplemental material.

Cys-scanning analyses. *E. coli* UT5600 cells carrying plasmids encoding each of the $BvgS^t$ Cys variants were grown in LB medium at 37°C under rotary shaking (220 rpm) for approximately 3 h 30 min to reach an optical density at 600 nm (OD_{600}) of ≥1.4. The cells were harvested by centrifugation and resuspended in M9 medium, supplemented when indicated with 5 mM chloronicotinate. After 30 min of incubation at 37°C with rotary shaking, the cells were treated for 10 min with 100 μM copper-*o*-phenanthroline and then for 5 min with 10 mM EDTA. The cells were harvested by centrifugation and resuspended at 17 OD_{600} per ml in 50 mM sodium phosphate (pH 6.8), 10 mM EDTA, 10 mM *N*-ethylmaleimide (NEM; Sigma) with 10 μg/ml DNase I and Complete EDTA-free protease inhibitor cocktail (Roche). The bacteria were lysed

Downloaded from http://mbio.asm.org/ on March 17, 2021 by guest

using a Hybaid Ribolyser apparatus (50 s at speed 6), and membrane proteins were harvested from the clarified lysates by ultracentrifugation at 90,000 × *g* for 1 h at 8°C. The pellets were resuspended in 100 μl sodium phosphate (50 mM, pH 6.8) and 33.3 μl lithium dodecyl sulfate (LDS) sample buffer (4×) (NuPAGE, Life Technologies) and heated at 70°C for 10 min. Electrophoresis was performed at a constant voltage of 150 V for 1 h in Tris-acetate-SDS running buffer using 3-to-8% Tris-acetate gels (NuPAGE Novex; Life Technologies). After electrotransfer of the proteins onto a nitrocellulose membrane and blocking with 5% skimmed milk, BvgS was detected by immunoblotting using antibodies raised against a 6-His tag (1:2,500 dilution; Sigma) and anti-mouse IgG-horseradish peroxidase (HRP)-conjugated antibodies (1:50,000 dilution; Jackson ImmunoResearch). The blots were developed using the Amersham ECL prime Western blotting detection system (GE Healthcare) and analyzed using an Amersham Imager 600 (GE Healthcare Life Sciences) in automatic acquisition mode. The contrast was enhanced on each entire blot separately with Photoshop. Dimer ratios were determined using the ImageQuant TL software. Control electrophoresis of the bacterial membrane extracts under reducing conditions and immunoblotting confirmed that dimerization is mediated by S-S bond formation. The Cys-scanning experiments were performed at least two times for each position, and the results were reproducible.

Energy calculations. Ten models of coiled coil for each variant of the sequence (699-RAELLRELHDAKESADAANRA-719; Leu and Ala residues are underlined) were generated using CCBuilder (45), using the default parameters for parallel dimeric coiled coils. The first Arg residue was placed in the a register position. For the $BvgS_{\Delta PAS}$ variants, the modeled segments included all the residues between the TM segment and the KTTFLAT motif of the DHp domain (e.g., 19 residues for $BvgS_{\Delta PAS\text{-}R1}$). For each structural model, the strength of interactions between the helices involved in coiled coils was calculated using CoilCheck+ in default mode, which measures the strength of interactions between helices involved in coiled coils using standard energy calculations involving nonbonded and electrostatic interactions, including H bonds, salt bridges, and van der Waals energy terms (46). The sums of these interactions are expressed as pseudoenergy values, whose range has been standardized using known structural entries of coiled coils. The pseudoenergy was averaged for the 10 models of each coiled-coil candidate.

Other methods. β-Galactosidase assays were performed as described previously (12). They were performed with 3 different clones at different times, and the standard errors of the means were determined. For the detection of inactive BvgS variants in *B. pertussis*, the bacteria were lysed, and the membrane proteins were harvested by ultracentrifugation as described above. Note that for the Cys variants, 10 mM NEM was added to the resuspended pellet before lysis. Electrophoresis and immunoblotting were performed as described above, except that the primary antibodies against BvgS were used (39) at a 1:2,000 dilution. The secondary antibodies (anti-rat HRP-conjugated antibodies; Abcam) were diluted to 1:10,000.

SUPPLEMENTAL MATERIAL

Supplemental material for this article may be found at http://mbio.asm.org/lookup/suppl/doi:10.1128/mBio.02089-15/-/DCSupplemental.

Text S1, DOCX file, 0.1 MB.
Figure S1, DOCX file, 1 MB.
Figure S2, DOCX file, 0.8 MB.
Figure S3, DOCX file, 0.2 MB.
Figure S4, DOCX file, 0.2 MB.
Figure S5, DOCX file, 0.1 MB.

ACKNOWLEDGMENTS

We thank Emmanuelle Petit and Justine Ecotière for help with mutagenesis and plasmid construction and René Wintjens for his critical reading of the manuscript.

E.L. was supported by a doctoral fellowship from the Region Nord-Pas-de Calais and INSERM. This work was supported by ANR-13-BSV8-0002-01 to F.J.-D. The funders had no role in designing the experiments or analyzing the data.

FUNDING INFORMATION

This work, including the efforts of Francoise Jacob-Dubuisson, was funded by Agence Nationale de la Recherche (ANR) (ANR-13-BSV8-0002-01).

The funders had no role in study design, data collection and interpretation, or the decision to submit the work for publication

REFERENCES

1. **Beier D, Gross R.** 2006. Regulation of bacterial virulence by two-component systems. Curr Opin Microbiol **9:**143–152. http://dx.doi.org/10.1016/j.mib.2006.01.005.
2. **Bekker M, Teixeira de Mattos MJ, Hellingwerf KJ.** 2006. The role of two-component regulation systems in the physiology of the bacterial cell. Sci Prog **89:**213–242. http://dx.doi.org/10.3184/003685006783238308.
3. **Hoch JA.** 2000. Two-component and phosphorelay signal transduction. Curr Opin Microbiol **3:**165–170. http://dx.doi.org/10.1016/S1369-5274(00)00070-9.
4. **Stock AM, Robinson VL, Goudreau PN.** 2000. Two-component signal transduction. Annu Rev Biochem **69:**183–215. http://dx.doi.org/10.1146/annurev.biochem.69.1.183.
5. **Kim JR, Cho KH.** 2006. The multi-step phosphorelay mechanism of unorthodox two-component systems in *E. coli* realizes ultrasensitivity to stimuli while maintaining robustness to noises. Comput Biol Chem **30:**428–444.
6. **Cotter PA, DiRita VJ.** 2000. Bacterial virulence gene regulation: an evolutionary perspective. Annu Rev Microbiol **54:**519–565. http://dx.doi.org/10.1146/annurev.micro.54.1.519.
7. **Cotter PA, Jones AM.** 2003. Phosphorelay control of virulence gene expression in *Bordetella*. Trends Microbiol **11:**367–373. http://dx.doi.org/10.1016/S0966-842X(03)00156-2.
8. **Jacob-Dubuisson F, Wintjens R, Herrou J, Dupré E, Antoine R.** 2012. BvgS of pathogenic *Bordetellae*: a paradigm for sensor kinase with Venus flytrap perception domains, p 57–83. In Gross R, Beier D (ed), Two-component system in bacteria. Caister Academic Press, Norfolk, United Kingdom.
9. **Dupré E, Herrou J, Lensink MF, Wintjens R, Vagin A, Lebedev A, Crosson S, Villeret V, Locht C, Antoine R, Jacob-Dubuisson F.** 2015. Virulence regulation with Venus flytrap domains: structure and function of the periplasmic moiety of the sensor-kinase BvgS. PLoS Pathog **11:**e1004700. http://dx.doi.org/10.1371/journal.ppat.1004700.
10. **Quiocho FA, Ledvina PS.** 1996. Atomic structure and specificity of bacterial periplasmic receptors for active transport and chemotaxis: variation of common themes. Mol Microbiol **20:**17–25. http://dx.doi.org/10.1111/j.1365-2958.1996.tb02484.x.
11. **Sobolevsky AI, Rosconi MP, Gouaux E.** 2009. X-ray structure, symmetry and mechanism of an AMPA-subtype glutamate receptor. Nature **462:**745–756. http://dx.doi.org/10.1038/nature08624.
12. **Dupré E, Lesne E, Guérin J, Lensink MF, Verger A, de Ruyck J, Brysbaert G, Vezin H, Locht C, Antoine R, Jacob-Dubuisson F.** 2015. Signal transduction by BvgS sensor-kinase: binding of modulator nicotinate affects conformation and dynamics of entire periplasmic moiety. J Biol Chem **290:**23307–23319. http://dx.doi.org/10.1074/jbc.M115.655720.
13. **Coote JG.** 1991. Antigenic switching and pathogenicity: environmental effects on virulence gene expression in *Bordetella pertussis*. J Gen Microbiol **137:**2493–2503. http://dx.doi.org/10.1099/00221287-137-11-2493.
14. **Lacey BW.** 1960. Antigenic modulation of *Bordetella pertussis*. J Hyg **58:**423–434. http://dx.doi.org/10.1017/S0022172400038134.
15. **Melton AR, Weiss AA.** 1993. Characterization of environmental regulators of *Bordetella pertussis*. Infect Immun **61:**807–815.
16. **Nakamura MM, Liew SY, Cummings CA, Brinig MM, Dieterich C, Relman DA.** 2006. Growth phase- and nutrient limitation-associated transcript abundance regulation in *Bordetella pertussis*. Infect Immun **74:**5537–5548. http://dx.doi.org/10.1128/IAI.00781-06.
17. **Herrou J, Bompard C, Wintjens R, Dupré E, Willery E, Villeret V, Locht C, Antoine R, Jacob-Dubuisson F.** 2010. Periplasmic domain of the sensor-kinase BvgS reveals a new paradigm for the Venus flytrap

Downloaded from http://mbio.asm.org/ on March 17, 2021 by guest

mechanism. Proc Natl Acad Sci U S A **107:**17351–17355. http://dx.doi.org/10.1073/pnas.1006267107.
18. **Ferris HU, Coles M, Lupas AN, Hartmann MD.** 2014. Crystallographic snapshot of the *Escherichia coli* EnvZ histidine kinase in an active conformation. J Struct Biol **186:**376–379. http://dx.doi.org/10.1016/j.jsb.2014.03.014.
19. **Marina A, Waldburger CD, Hendrickson WA.** 2005. Structure of the entire cytoplasmic portion of a sensor histidine-kinase protein. EMBO J **24:**4247–4259.
20. **Mechaly AE, Sassoon N, Betton JM, Alzari PM.** 2014. Segmental helical motions and dynamical asymmetry modulate histidine kinase autophosphorylation. PLoS Biol **12:**e1001776. http://dx.doi.org/10.1371/journal.pbio.1001776.
21. **Perraud AL, Rippe K, Bantscheff M, Glocker M, Lucassen M, Jung K, Sebald W, Weiss V, Gross R.** 2000. Dimerization of signalling modules of the EvgAS and BvgAS phosphorelay systems. Biochim Biophys Acta **1478:**341–354. http://dx.doi.org/10.1016/S0167-4838(00)00052-2.
22. **Wang C, Sang J, Wang J, Su M, Downey JS, Wu Q, Wang S, Cai Y, Xu X, Wu J, Senadheera DB, Cvitkovitch DG, Chen L, Goodman SD, Han A.** 2013. Mechanistic insights revealed by the crystal structure of a histidine kinase with signal transducer and sensor domains. PLoS Biol **11:**e1001493. http://dx.doi.org/10.1371/journal.pbio.1001493.
23. **Casino P, Rubio V, Marina A.** 2010. The mechanism of signal transduction by two-component systems. Curr Opin Struct Biol **20:**763–771. http://dx.doi.org/10.1016/j.sbi.2010.09.010.
24. **Bhate MP, Molnar KS, Goulian M, DeGrado WF.** 2015. Signal transduction in histidine kinases: insights from new structures. Structure **23:**981–994. http://dx.doi.org/10.1016/j.str.2015.04.002.
25. **Molnar KS, Bonomi M, Pellarin R, Clinthorne GD, Gonzalez G, Goldberg SD, Goulian M, Sali A, DeGrado WF.** 2014. Cys-scanning disulfide crosslinking and Bayesian modeling probe the transmembrane signaling mechanism of the histidine kinase, PhoQ. Structure **22:**1239–1251. http://dx.doi.org/10.1016/j.str.2014.04.019.
26. **Herrou J, Debrie AS, Willery E, Renauld-Mongénie G, Locht C, Mooi F, Jacob-Dubuisson F, Antoine R.** 2009. Molecular evolution of the two-component system BvgAS involved in virulence regulation in *Bordetella*. PLoS One **4:**e6996. http://dx.doi.org/10.1371/journal.pone.0006996.
27. **Woolfson DN.** 2005. The design of coiled-coil structures and assemblies. Adv Protein Chem **70:**79–112. http://dx.doi.org/10.1016/S0065-3233(05)70004-8.
28. **Grigoryan G, Keating AE.** 2008. Structural specificity in coiled-coil interactions. Curr Opin Struct Biol **18:**477–483. http://dx.doi.org/10.1016/j.sbi.2008.04.008.
29. **Meier M, Stetefeld J, Burkhard P.** 2010. The many types of interhelical ionic interactions in coiled coils—an overview. J Struct Biol **170:**192–201. http://dx.doi.org/10.1016/j.jsb.2010.03.003.
30. **Möglich A, Ayers RA, Moffat K.** 2009. Design and signaling mechanism of light-regulated histidine kinases. J Mol Biol **385:**1433–1444. http://dx.doi.org/10.1016/j.jmb.2008.12.017.
31. **Jones AM, Boucher PE, Williams CL, Stibitz S, Cotter PA.** 2005. Role of BvgA phosphorylation and DNA binding affinity in control of Bvg-mediated phenotypic phase transition in *Bordetella pertussis*. Mol Microbiol **58:**700–713. http://dx.doi.org/10.1111/j.1365-2958.2005.04875.x.
32. **Ulrich LE, Zhulin IB.** 2007. Mist: a microbial signal transduction database. Nucleic Acids Res **35:**D386–D390. http://dx.doi.org/10.1093/nar/gkl932.
33. **Eguchi Y, Utsumi R.** 2014. Alkali metals in addition to acidic pH activate the EvgS histidine kinase sensor in *Escherichia coli*. J Bacteriol **196:**3140–3149. http://dx.doi.org/10.1128/JB.01742-14.
34. **Landschulz WH, Johnson PF, McKnight SL.** 1988. The leucine zipper: a hypothetical structure common to a new class of DNA binding proteins. Science **240:**1759–1764. http://dx.doi.org/10.1126/science.3289117.
35. **Saita E, Abriata LA, Tsai YT, Trajtenberg F, Lemmin T, Buschiazzo A, Dal Peraro M, de Mendoza D, Albanesi D.** 2015. A coiled coil switch mediates cold sensing by the thermosensory protein DesK. Mol Microbiol **98:**258–271. http://dx.doi.org/10.1111/mmi.13118.
36. **Manetti R, Aricò B, Rappuoli R, Scarlato V.** 1994. Mutations in the linker region of BvgS abolish response to environmental signals for the regulation of the virulence factors in *Bordetella pertussis*. Gene **150:**123–127. http://dx.doi.org/10.1016/0378-1119(94)90870-2.
37. **Miller JF, Johnson SA, Black WJ, Beattie DT, Mekalanos JJ, Falkow S.** 1992. Constitutive sensory transduction mutations in the *Bordetella pertussis bvgS* gene. J Bacteriol **174:**970–979.
38. **Johnson MD, Bell J, Clarke K, Chandler R, Pathak P, Xia Y, Marshall RL, Weinstock GM, Loman NJ, Winn PJ, Lund PA.** 2014. Characterization of mutations in the PAS domain of the EvgS sensor kinase selected by laboratory evolution for acid resistance in *Escherichia coli*. Mol Microbiol **93:**911–927. http://dx.doi.org/10.1111/mmi.12704.
39. **Dupré E, Wohlkonig A, Herrou J, Locht C, Jacob-Dubuisson F, Antoine R.** 2013. Characterization of the PAS domain in the sensor-kinase BvgS: mechanical role in signal transmission. BMC Microbiol **13:**172. http://dx.doi.org/10.1186/1471-2180-13-172.
40. **Perraud AL, Kimmel B, Weiss V, Gross R.** 1998. Specificity of the BvgAS and EvgAS phosphorelay is mediated by the C-terminal HPt domains of the sensor proteins. Mol Microbiol **27:**875–887. http://dx.doi.org/10.1046/j.1365-2958.1998.00716.x.
41. **Antoine R, Alonso S, Raze D, Coutte L, Lesjean S, Willery E, Locht C, Jacob-Dubuisson F.** 2000. New virulence-activated and virulence-repressed genes identified by systematic gene inactivation and generation of transcriptional fusions in *Bordetella pertussis*. J Bacteriol **182:**5902–5905. http://dx.doi.org/10.1128/JB.182.20.5902-5905.2000.
42. **Guédin S, Willery E, Tommassen J, Fort E, Drobecq H, Locht C, Jacob-Dubuisson F.** 2000. Novel topological features of FhaC, the outer membrane transporter involved in the secretion of the *Bordetella pertussis* filamentous hemagglutinin. J Biol Chem **275:**30202–30210. http://dx.doi.org/10.1074/jbc.M005515200.
43. **Eddy SR.** 2009. A new generation of homology search tools based on probabilistic inference. Genome Inform **23:**205–211.
44. **Finn RD, Bateman A, Clements J, Coggill P, Eberhardt RY, Eddy SR, Heger A, Hetherington K, Holm L, Mistry J, Sonnhammer EL, Tate J, Punta M.** 2014. Pfam: the protein families database. Nucleic Acids Res **42:**D222–D230. http://dx.doi.org/10.1093/nar/gkt1223.
45. **Wood CW, Bruning M, Ibarra AÁ, Bartlett GJ, Thomson AR, Sessions RB, Brady RL, Woolfson DN.** 2014. CCBuilder: an interactive web-based tool for building, designing and assessing coiled-coil protein assemblies. Bioinformatics **30:**3029–3035. http://dx.doi.org/10.1093/bioinformatics/btu502.
46. **Sunitha MS, Nair AG, Charya A, Jadhav K, Mukhopadhyay S, Sowdhamini R.** 2012. Structural attributes for the recognition of weak and anomalous regions in coiled-coils of myosins and other motor proteins. BMC Res Notes **5:**530. http://dx.doi.org/10.1186/1756-0500-5-530.

Downloaded from http://mbio.asm.org/ on March 17, 2021 by guest